

Heating of Heavy Ions by Interplanetary Coronal Mass Ejection (ICME) Driven Collisionless Shocks

K. E. Korreck^{1,2}, T. H. Zurbuchen², S. T. Lepri², & J. M. Raines²

ABSTRACT

Shock heating and particle acceleration processes are some of the most fundamental physical phenomena of plasma physics with countless applications in laboratory physics, space physics, and astrophysics. This study is motivated by previous observations of non-thermal heating of heavy ions in astrophysical shocks (Korreck et al. 2004). Here, we focus on shocks driven by Interplanetary Coronal Mass Ejections (ICMEs) which heat the solar wind and accelerate particles. This study focuses specifically on the heating of heavy ions caused by these shocks. Previous studies have focused only on the two dynamically dominant species, H^+ and He^{2+} . This study utilizes thermal properties measured by the Solar Wind Ion Composition Spectrometer (SWICS) aboard the Advanced Composition Explorer (ACE) spacecraft to examine heavy ion heating. This instrument provides data for many heavy ions not previously available for detailed study, such as Oxygen (O^{6+} , O^{7+}), Carbon (C^{5+} , C^{6+}), and Iron (Fe^{10+}). The ion heating is found to depend critically on the upstream plasma β , mass per charge ratio of the ion, M/Q , and shock magnetic angle, θ_{Bn} . Similar to past studies (Schwartz et al. 1988), there is no strong dependence of ion heating on Mach number. The heating mechanism described in Lee & Wu (2000) is examined to explain the observed heating trends in the heavy ion thermal data.

Subject headings: Sun: coronal mass ejections (CMEs) — acceleration of particles

1. Introduction

Shocks constitute a non-linear transition between two dynamically different plasma states. At this transition, a portion of the bulk flow energy of the plasma is transferred into thermal energy of its components. A very small fraction (1-10%) of the interacting plasma becomes highly energized and is injected into particle acceleration processes boosting the particles to very high energy ($E \geq GeV$). There is, however, a lack of understanding of the dynamic effects that lead to this heating. The heating of an ion species appears to be dependent on the ion properties as well as on the bulk properties of the shock and the initial state of the plasma (Shimada & Hoshino 2003; Lee & Wu 2000; Korreck et al. 2004; Berdichevsky et al. 1997). It is the purpose of this paper to investigate the heating of solar wind ions using accessible thermal data of heavy ions from shocks driven

by the interplanetary manifestations of Coronal Mass Ejections (CMEs) - Interplanetary CMEs (ICMEs).

Lee & Wu (2000) discuss three parameters key to understanding heating in collisionless shocks: Alfvénic Mach number, M_A , magnetic shock angle, θ_{Bn} , and upstream plasma β , the ratio of thermal to magnetic energy. The dependence of heating on these parameters has been examined before in solar wind shocks both observationally and theoretically (Ogilvie et al. 1980; Zertsalov et al. 1976; Berdichevsky et al. 1997; Zhao et al. 1991). Work by Berdichevsky et al. (1997) examined the heating of ions in the solar wind. The heating of heavy ions such as O^{6+} was found to be more than mass proportional when compared to the heating of protons. This appears to contradict heating seen in other shocks such as those around supernova remnants (Korreck et al. 2004). The Berdichevsky et al. (1997) paper also found the ion heating to be most efficient when the initial

¹Harvard Smithsonian Center for Astrophysics, 60 Garden Street, Cambridge, MA 02138

²University of Michigan, Atmospheric, Oceanic, and Space Science Department, Ann Arbor, MI 48109

ion and proton thermal velocity were similar, i.e. energy is distributed mass proportionally.

The effect of Alfvénic Mach number of the shock on heating has been studied observationally in the heliosphere. The Alfvénic Mach number is used instead of the acoustic Mach number due to the magnetic nature of the solar wind. Schwartz et al. (1988) used data from crossings of the Earth's bow shock to study the heating of ions and electrons. Only a weak correlation between increasing Mach number and decreased heating was found.

The plasma β is a defining characteristic of the plasma. For example, Lipatov & Zank (1999) found for plasmas with $\beta \geq 0.1$ ions were unable to "surf" waves as an acceleration process, making plasma β a determining factor in particle acceleration models. Note that in the heliosphere β is normally ≤ 1.0 (Galvin 1997).

The magnetic angle from the shock normal, θ_{Bn} , has also been examined with respect to the acceleration of ions. Quasi-parallel shocks have been shown to accelerate ions from thermal energies to well above what would be expected from the bulk energy transfer (Ellison 1981; Scholer 1990; Giacalone et al. 1992; Kucharek & Scholer 1995). Quasi-perpendicular shocks have been shown to be inefficient for accelerating ions from thermal ion populations, however these shocks are the most efficient accelerators if there is a seed population available. The acceleration efficiency, once the seed population is available, is inversely proportional to θ_{Bn} (Ellison et al. 1995); the more perpendicular the shock, the more efficient the acceleration. Hence, in order to understand cosmic ray acceleration, the heating of a suprathermal seed particle population is of great importance.

In addition to the three parameters mentioned above, the mass-to-charge ratio also plays a crucial role in heating of heavy ions. As the mass-to-charge ratio increases the heating of ions increases (Lee & Wu 2000). The mass-to-charge ratio dictates which types of MHD wave interactions are available to the particles at the shock front.

The novel data on ICMEs from the Advanced Composition Explorer (ACE) spacecraft (Stone et al. 1998) afford us the opportunity to study these shocks and the heating processes for individual ion species in greater detail. While the previous work included only protons, helium, and

oxygen (O^{6+}) in the analysis, this study is extended to include O^{7+} , C^{5+} , C^{6+} , and Fe^{10+} ions, extending the mass-to-charge ratio range to 1 thru 5.6.

This paper examines the heating of heavy ions with respect to all critical parameters mentioned above that dominate shock heating - the magnetic shock geometry - θ_{Bn} , Alfvénic Mach number - M_A , plasma β , and M/Q , the mass per charge ratio. We utilize thermal properties measured by the Solar Wind Ion Composition Spectrometer (SWICS) (Gloeckler et al. 1998) on the ACE spacecraft. We characterize a statistically significant sample of 20 shocks for which heavy ion heating is observed with high statistical accuracy and with well-defined shock properties. Magnetic field data from the Magnetometer (MAG) instrument (Smith et al. 1998) and proton data from the Solar Wind Electron Proton Alpha Monitor (SWEPAM) instrument (McComas et al. 1998) were also used.

The plasma data available from the ACE spacecraft and a brief discussion of errors are described in Section 2. The selection of ICME shocks is discussed in Section 3. In Section 4, the heating of ions is examined with respect to each parameter. A method of heating is described in Section 5 and conclusions are summarized in Section 6.

2. Observations

The ACE spacecraft, launched in 1997, orbits about the first Lagrangian, L1 point, 235 Earth radii upstream along the Sun-Earth line. Three of the nine instruments aboard were used for this study. The SWICS, MAG, and SWEPAM instruments provide data on ion composition, velocity, density, and the ambient magnetic field. For this study, the following physical quantities were analyzed: proton temperature, proton thermal velocity, proton number density, thermal velocities of He^{2+} , O^{6+} , O^{7+} , C^{5+} , C^{6+} , and Fe^{10+} , and magnetic field.

The heavy ion data ($Z>1$) was obtained from the SWICS instrument. This instrument is composed of an electrostatic analyzer, which measures an ion's energy per charge, and a time-of-flight-energy telescope, which measures an ion's velocity and total energy. The combination of these two sensors enables unique identification of a particle's

mass, charge, and energy (Gloeckler et al. 1998). For this study, we use SWICS data with 1-hour time resolution; this time resolution provides sufficient statistics for the minor ions studied. For each one hour time bin, five 12-minute accumulation cycles were summed. Care has been taken to exclude the accumulation cycle that contains the moment of the shock passage, because it mixes upstream and downstream distributions. The proton thermal velocity, the proton number density, and the magnetic field data were taken from the combined SWEPPAM/MAG data set available on the web at:

<http://www.srl.caltech.edu/ACE/ASC/>. 64-second averages of data were used. The data from each physical quantity were averaged for one hour before or one hour after the shock. This allows for a relatively local measurement of the shock, but statistically significant heavy ion data. There are important statistical limits to these data, which are discussed in section 2.1.

2.1. Errors

For the proposed heating analysis, it is necessary to quantify the thermal width, or thermal speed, of the heavy ion distributions. However, the thermal speed is only defined if distributions are Gaussian. We have therefore implemented a test of the fit of a Gaussian to the data using the following technique. For each heavy ion measurement, the thermal speed was calculated using two techniques: by calculating the second moment of the observed distribution, v_{th} , and by determining the thermal speed by least-squares fit of a Gaussian to the distribution, $v_{th,fit}$. The deviations between these two quantities are a measure of the deviations of the distributions from a Gaussian shape.

The deviations were relatively small for most ions with an average value of $<10\%$, but we do find a few examples for which energetic tails on the distribution function dominate, and the error on v_{th} was then increased, to a more conservative error estimate of 20% in order to account for this.

In order to combine plasma data with our composition-resolved dynamics data, we averaged the necessary solar wind parameters for 1 hour ahead of and behind the shock front using data taken at intervals of 64 seconds, to overlap with the SWICS data-interval. The statistical error was

then calculated as the standard deviation of each averaged quantity.

3. Shock Selection

Shocks were selected from the Cane & Richardson (2003) list of ICMEs and the ACE Shock List maintained online¹. The ACE Shock List details the time of the shock passage, the angle between upstream magnetic field vector and the shock normal, θ_{Bn} , and the upstream Mach number, M_A

The first criterion for selecting a shock for this study was to have all crucial data-sets available for two hours before and two hours after the shock passage. The next criterion for selection was the characteristics of the kinetic temperature of the solar wind before the shock passage. Since the kinetic temperature of the solar wind provides a measure of the shock and the plasma characteristics upstream and downstream of the shock, an increase in temperature before the time of the shock indicates pre-heating, ion feedback or a reverse shock (Paschmann et al. 1981; Gloeckler 1999). The presence of these features would bias the study since ions are heated differently, hence these instances need to be excluded. If the temperature increased in the time period between 60 to 30 minutes prior to the shock passage by more than 30% of the mean value of the temperature calculated up to 30 minutes before the shock, the shock was considered to exhibit pre-heating and was excluded from the analysis.

Representative solar wind parameters for an ICME shock are plotted versus time in Figure 1. Panel A shows the solar wind proton velocity, v_p , versus time as the solid line and the velocity of each heavy ion is included as a different symbol, as indicated in the plot legend. Panel B shows the proton number density, n , in the solar wind. Panel C is a plot of the thermal velocity, v_{th} , of protons with the over-plotted symbols representing the thermal velocity of individual ions. Panel D plots the solar wind proton temperature, T_p , versus time. Panel E contains the magnitude of the magnetic field, B , versus time. Panel F is a plot of the magnetic latitude, δ , and longitude, λ , versus time.

¹

[http://www.bartol.udel.edu/\\$\sim\\$chuck/ace/ACElists/obs_list.html](http://www.bartol.udel.edu/\simchuck/ace/ACElists/obs_list.html)

In order to examine the dependence of heating on shock orientation with respect to the background magnetic field, the shock list was broken up into quasi-parallel and quasi-perpendicular shocks. Quasi-parallel shocks were defined to have θ_{Bn} between 0 and 20 degrees and shocks with θ_{Bn} between 80 and 90 degrees were considered quasi-perpendicular. There were 16 quasi-perpendicular shocks available for study and 4 quasi-parallel shocks. In subsequent sections, each parameter will be explored for a perpendicular and parallel shock separately.

4. Heavy Ion Heating

There are two methods of heating ions that are widely invoked in the study of collisionless shocks. First, the transfer of the bulk fluid kinetic energy to the thermal energy of the particles leading to mass proportional heating or all ions having the same velocity. The second method is wave particle interactions that would result in a M/Q dependence in heating.

Another point of interest is the distribution of heating among the different ion species. In studies in the heliosphere (Berdichevsky et al. 1997), it was found that ions are heated more than mass proportionally than ions. However, in studies of the collisionless shocks in supernova remnants, the ions are heated less than mass proportionally to the protons (Korreck et al. 2004). Lee & Wu (2000) found that the heavy ions are heated by direct transmission through the shock as reflection of heavy ions by the shock potential is prohibitive due to their large mass.

In order to determine which mechanism or mechanisms are responsible for the heating, we first quantify the heating of each ion species, including protons, and then examine the heating dependence on M/Q, M_A , and β to try to elucidate a candidate mechanism for heating.

In this study the heating, H , of an ion at a shock is defined as the ratio of the square of the upstream and downstream thermal velocities.

$$H = \frac{v_{th_d}^2}{v_{th_u}^2} = \frac{3kT_{s,d}/m_s}{3kT_{s,u}/m_s} = \frac{T_{s,d}}{T_{s,u}} \quad (1)$$

where

T_s = Temperature of the species

m_s = Mass of the species

v_{th_d} = Average thermal velocity of the species one hour downstream

v_{th_u} = Average thermal velocity of the species one hour upstream

k = Boltzmann constant

However, it has been recognized that the solar wind is not initially in thermal equilibrium: heavy ions have a tendency to exhibit high kinetic temperatures, (Hefti et al. 1998; Zurbuchen et al. 2000; von Steiger & Zurbuchen 2003). In order to accurately describe the ion heating, the preshock temperature ratio of ion temperature to proton temperature needs to be considered. The ratio of preshock ion to proton temperature shows only one of the 96 data points to be significantly less than 1. The data in general supports an initial condition where ions have equal if not higher thermal speeds than the protons. Therefore, relative heating ratios based on initial thermal speeds will give the clearest quantification of heating through the shock passage.

Examining the current data set with respect to the temperature ratio of the downstream ions to protons, we have found that the heating is on average less than mass proportional for the ions except Fe^{+10} , although 27 out of the 96 data points for perpendicular shocks did show greater than mass proportional heating. This contradicts earlier studies by Berdichevsky et al. (1997) that found all of the ion heating to be greater than mass proportional.

The heating of the ions are plotted versus the initial temperature ratio of the ion to the proton in Figures 2a and 2b. The values of initial ratio are all greater than or equal to one except for one data point. The heating, if greater than one, indicates that the species was heated through the shock. However, only 69% of the ions were heated in the perpendicular shocks and 70% in the parallel shocks. The others actually showed a decrease in temperature across the shock front. Protons all gained heat or maintained their temperature across the shock front.

In Figures 3a and 3b, the ratio of ion and proton heating, H_i/H_p , is plotted versus the initial ratio of thermal speeds of the ion and proton where H_p is the heating ratio for protons. Only 43% of the ions in perpendicular shocks were heated more than the protons and 50% of those ions in parallel

shocks. The protons are therefore gaining more heat than the ions in these shocks.

To characterize the heating mechanism consistent with the current data set, the dependence of the heating on Alfvénic Mach number, M_A , plasma β , and mass to charge ratio, M/Q , for both quasi-parallel and quasi-perpendicular shocks will now be examined.

4.1. Dependence of Heating on Alfvénic Mach Number

Shocks can heat ions by converting bulk kinetic energy into thermal kinetic energy of the particles. The Mach number gauges the speed of the propagation of bulk fluid flow relative to the surrounding medium. The Mach number used in this study is the Alfvénic Mach number, which takes into account interaction with the surrounding magnetized plasma. Previous studies, (Schwartz et al. 1988) showed the collisionless heating to be weakly dependent on Mach number.

The method of energy transfer can be determined by the Critical Mach number. Below an Alfvénic Mach number of approximately 2 (Kennel 1987), also called a sub-critical shock, the effective dissipation of energy by the shock is local, i.e. the heating is spatially local to the shock front via conduction. Above this critical Mach number the dissipation is based on multiple streams of ions which have longer characteristic scales. A convenient measure of a supercritical shock is the ratio of the Alfvénic to Magnetosonic Mach numbers. If this ratio is ≥ 1 then the shock is supercritical by this definition. We have calculated that all the shocks in this study are supercritical. The data therefore implies a heating method that involves wave particle interaction. Protons heating has been shown to result from both direct transmission and reflected protons in these supercritical shocks (Lee et al. 1987).

Figure 4a, shows the Alfvénic Mach number versus the heating for quasi-perpendicular shocks. The heating, H , is described by Equation 1. The line shows a linear fit to the data with an increasing trend. The parallel fit seems kinked due to the logarithmic scale for the data. The quasi-parallel shocks in Figure 4b also shows an increasing trend with increasing Mach number however with a smaller data set and less statistics it seems

to be a weaker effect. This contradicts the findings of Schwartz et al. (1988), however the fits are marginal ($\chi^2_\nu \sim 5$ for the parallel fit and 0.6 for the perpendicular fit).

4.2. Plasma β Effect on Heating

Plasma β is plotted versus the heating for each ion species for perpendicular shocks in Figure 5a. The plot shows that with increasing β the heating of the ions decreases. The heating is therefore more effective in magnetically dominated regimes. The lines plotted are the fit to an exponential fit to the data.

For the parallel shocks, Figure 5b, there is an observed decrease in heating with increasing β , however, only a few shocks are available for study and hence the trend is more uncertain but decreases more sharply than the perpendicular shocks.

4.3. Heating and Mass to Charge Ratio

The mass to charge ratio of an ion determines the type of wave and particle interaction that the ion can experience. In Figures 6a and 6b, the average heating per ion is plotted versus the mass to charge ratio for perpendicular and parallel shocks respectively. The line is a least squared fit to the mean values with the standard deviation of the mean values as error bars. For the perpendicular shock the fit has a reduced chi-squared value of $\chi^2_\nu=0.25$, for the expression $H=1.15+01.6M/Q$. The fit for the parallel shocks, $\chi^2_\nu \sim 0.48$, the line is present to emphasize the trend towards an increase in heating with increasing M/Q ratio.

In the perpendicular shocks both the $M/Q=2$ ions are heated approximately the same, whereas in the parallel shocks they are heated differently, making the mass important in the parallel shock given that the larger value is the C^{6+} ion, where the M/Q ratio is important for the perpendicular shock.

These shock exhibit an increase in heating based on a larger M/Q ratio regardless of the exact θ_{Bn} , however, the effect is more pronounced in the perpendicular shock. Lee & Wu (2000) found that due to transmission of ions across the shock, the gyro speed, v_g , is approximately equal to the thermal speed. The gyro speed increased as the M/Q ratio increased which agrees with this data

set.

5. Discussion of Heating Mechanisms

A shock heating mechanism is needed that addresses all observational constraints found in this study. Any proposed mechanism must meet the following criteria:

1. Heating increases with decreasing β
2. Perpendicular shocks heat more effectively than parallel shocks
3. The ions that initially have thermal velocities nearly equal to protons are preferentially heated
4. Heating increases with increasing mass-to-charge ratio.
5. Increasing Mach Number increases the heating

Lee & Wu (2000) modeled heating in the solar corona. This heating mechanism and the predictions for the downstream thermal speed will be used to evaluate this mechanism for the CME shock heating. The protons are the main species and will form the shock while the heavy ions will act as test particles through the shock front. The simplifying assumption will be made that all changes in the ions velocity will occur parallel to the shock normal. The proton speed is also assumed to be the speed of the solar wind or the upstream bulk speed. As protons pass through the shock they are slowed according to the Rankine-Hugoniot conditions in order to conserve energy. Their bulk kinetic energy is changed into potential energy forming an effective electrostatic potential. Therefore, the potential is proportional to the change in energy of the proton.

$$q\phi \sim \frac{1}{2}m_p v_{p,u}^2 - \frac{1}{2}m_p v_{p,d}^2 \quad (2)$$

This potential jump is seen by the heavy ions as they approach the shock front. But the heavy ions conserve energy, increasing their velocity across the shock according to their M/Q ratio.

$$\Delta K.E._i = q_i \phi = \frac{1}{2}m_i(v_{i,u}^2 - v_{i,d}^2) \quad (3)$$

where q_i is the charge of the ion, m_i is the mass of the ion in units of proton mass, $v_{i,u}$ is the velocity of the ion upstream and $v_{i,d}$ is the velocity of the ion downstream of the shock. Plugging in the potential formed by the protons (2) to the kinetic energy of the heavy ions (3), we can find an expression for the downstream ion velocity in terms of the M/Q (α) and observed parameters.

$$v_{i,d} = v_p \sqrt{\frac{(\alpha - 1) + c^2}{\alpha}} \quad (4)$$

where α is the mass to charge ratio, v_p is the solar wind proton velocity, and c is the ratio of downstream proton velocity to upstream proton velocity in the shock frame.

The velocity computed in Equation 4 is the kinetic velocity of the particle at the shock front. However, we are trying to examine the thermal speed of the heavy ions. As the distribution of the ions moves away from Maxwellian, the thermal speed becomes a measure of kinetic energy. Lee & Wu (2000) derived that for a perpendicular shock the gyro velocity was approximately equal to the thermal velocity. Using the definition of gyro velocity from the Lee & Wu (2000) paper,

$$v_{i,d,th} = v_{gyro} = v_{p,u} \left| \sqrt{\left(1 - \frac{\alpha Q}{M}\right)} - \frac{B_{t,1}}{B_{t,2}} \right| \quad (5)$$

where α is defined as $e\Delta\phi/\epsilon_0$ - the ratio of electric potential at the shock front to the kinetic energy of protons upstream, $v_{p,u}$ is the upstream solar wind proton velocity, $B_{t,1}$ is the upstream magnitude of the tangential magnetic field, and $B_{t,2}$ is the downstream magnitude of the tangential magnetic field.

By inspection, the downstream thermal velocity does increase with increasing M/Q ratio. Using the definition of a Mach number the relationship between the upstream proton velocity and the Mach number is found to be $v_{p,u} = M_A v_A$. Inserting this relation into the square of Equation 5 in order to compare with the ion heating data, the heating of the ions is proportional to the square of the Mach number. However, in the actual data sets, there is an increase of heating with respect to increasing Mach number however not a significant heating as suggested by this equation.

The plasma β is inversely correlated with the square of the Alfvén velocity. With respect to

plasma β the data match the predicted trend of Equation 5 as the heating decreased with increasing β .

As the Mach number increases we expect to have greater shock compression of the magnetic field which would lead to a larger $B_{t,2}$. The Mach number is not as strongly correlated as the magnetic characteristics, such as θ_{Bn} or β , with the heating of the heavy ions, however, the bulk motion provided by shocks at higher Mach numbers is necessary for the compression of downstream magnetic fields that influence the gyro velocity.

6. Conclusions

This study examined different ion species in the solar wind to investigate the heating that occurs at a collisionless shock front ahead of ICMEs. Based on the magnetic field angle to the shock normal, θ_{Bn} , each shock was analyzed for its dependence on Mach number, M_A , plasma β , and the behavior of ions based on their mass to charge ratio, M/Q . An increasing β was found to reduce the ion heating at the shock, highlighting the importance of the magnetic field to the heating process. As the Mach number increased the heating also increased. As the mass to charge ratio increases, the heating of the ion increases. Quasi-perpendicular shocks were shown to heat the ions more efficiently than the quasi-parallel shocks.

A heating method based on a post-shock potential described by Lee & Wu (2000) was examined for the heating trends observed in this study. The data and the predicted values of heating were not well correlated for the parallel shock but did match trends found for the M/Q , M_A and plasma β trends for the perpendicular shocks. The mechanism reveals an increased heating with increasing Mach number. However, the magnitude of the increase in heating with Mach number is not of the same order of magnitude that is found in the data and the trend however weak is inverse to that found by Schwartz et al. (1988).

There is currently similar ion heating data available for collisionless shocks in supernova remnants showing non-preferential heating to ions. Using the data compiled here we can compare the heating ratios of ions to protons downstream and use that ratio to find a plasma β for the supernova remnant (SNR). In Korreck et al. (2004), it was

found that the ratio of oxygen to proton temperature post-shock was 8.3. Using the fit of heating versus plasma β for the CME data, we obtain a β for SN1006 of 1.7. Knowing the temperature, $T=1.5 \times 10^9 \text{ K}$, and the density given, 0.25 cm^{-3} , we can also find a magnetic field of $1 \mu\text{Gauss}$. This is very close to the assumed galactic magnetic field of $3 \mu\text{Gauss}$. These types of diagnostics could lead to a better understanding of the magnetic field in SNRs and their role in ion heating and acceleration.

This begs the question of the ubiquitous nature of the shock physics: what is the dominant factor to determine effect heating at a collisionless shock front? The supernova has a Mach number 10 times that of the CME shocks however, as seen in this data set, the Mach number is not the only factor in determining heating. Density and magnetic energy seem to be of greater importance.

The ACE science center is found at <http://www.srl.caltech.edu/>. This work was performed with the support of ACE contract number. K. Korreck acknowledges the Rackham-NSF Fellowship for funding this work. This work made use of NASA's Astrophysical Data System.

Facilities: ACE.

REFERENCES

- Berdichevsky, D., Geiss, J., Gloeckler, G., & Mall, U. 1997, J. Geophys. Res., 102, 263
- Cane, H. & Richardson, I. 2003, J. Geophys. Res., 108, 1156
- Ellison, D.C. 1981, Geophys. Res. Lett., 8, 991
- Ellison, D.C., Baring, M.G., & Jones, F.C. 1995, ApJ, 453, 873
- Galvin, A.B. 1997, in *Coronal Mass Ejections*, ed. N. Crooker, J.A. Joselyn, & J. Feynman, *Geophys. Monograph*, 99, 253
- Giacalone, J., Burgess, D., Schwartz, S.J., & Ellison, D.C. 1992, Geophys. Res. Lett., 19, 433
- Gloeckler, G. 1999, Space Science Reviews, 89, 91
- Gloeckler, G., Cain, J., Ipavich, F.M., Tums, E.O., Bedini, P., Fisk, L.A., Zurbuchen,

T.H., Bochsler, P., Fischer, J., Wimmer-Schweingruber, R.F., Geiss, J., & Kallenbach, R. 1998, Space Science Reviews, 86, 497

Hefti, S., et al. 1998, J. Geophys. Res., 103, 29697

Kennel, C.F. 1987, J. Geophys. Res., 92, 13427

Korreck, K.E., Raymond, J.C., Zurbuchen, T.H., Ghavamian, P. 2004, ApJ, 615, 280

Kucharek, H. & Scholer, M. 1995, J. Geophys. Res., 100, 1745

Lee, L. C., Mandt, M. E., & Wu, C. S. 1987, J. Geophys. Res., 92, 13438

Lee, L. & Wu, B. 2000, ApJ, 535, 1014

Lipatov, A.S. & Zank, G.P. 1999, Physical Review Letters, 82, 3609

McComas, D.J., Bame, S.J., Barker, P., Feldman, W.C., Phillips, J.L., Riley, P., & Griffee, J.W. 1998, Space Science Reviews, 86, 563

Ogilvie, K.W., Bochsler, P., Geiss, J., & Coplan, M.A. 1980, J. Geophys. Res., 85(14), 6069

Paschmann, G., Sckopke, N., Papamastorakis, I., Asbridge, J. R., Bame, S. J., & Gosling, J. T. 1981, J. Geophys. Res., 86, 4355

Scholer, M. 1990, Geophys. Res. Lett., 17, 1821

Schwartz, S.J., Thomsen, M.F., Bame, S.J., Stansberry, J. 1988, J. Geophys. Res., 93(A11), 12, 923

Shimada, N. & Hoshino, M. 2003, International Cosmic Ray Conference, 4, 2421

Smith, C.W., L'Heureux, J., Ness, N.F., Acuna, M.H., Burlaga, L.F., Scheifele, J. 1998, Space Science Reviews, 86, 613

Stone, E.C., Frandsen, A.M., Mewaldt, R.A., Christian, E.R., Margolies, D., Ormes, J.F., & Snow, F. 1998, Space Science Reviews, 86, 1-22

von Steiger, R. & Zurbuchen, T.H. 2003, AIP Conf. Proc. 679: Solar Wind Ten, 679, 526

Zertsalov, A.A., Vaisberg, O.L., Temnyi, V.V. 1976, Cosmological Research, 14, 257

Zhao, X., Ogilvie, K.W., Whang, Y.C. 1991, J. Geophys. Res., 96, 5437

Zurbuchen, T.H., Fisk, L.A., Schwadron, N.A., & Gloeckler, G. 2000, AIP Conf. Proc. 528: Acceleration and Transport of Energetic Particles Observed in the Heliosphere, 215

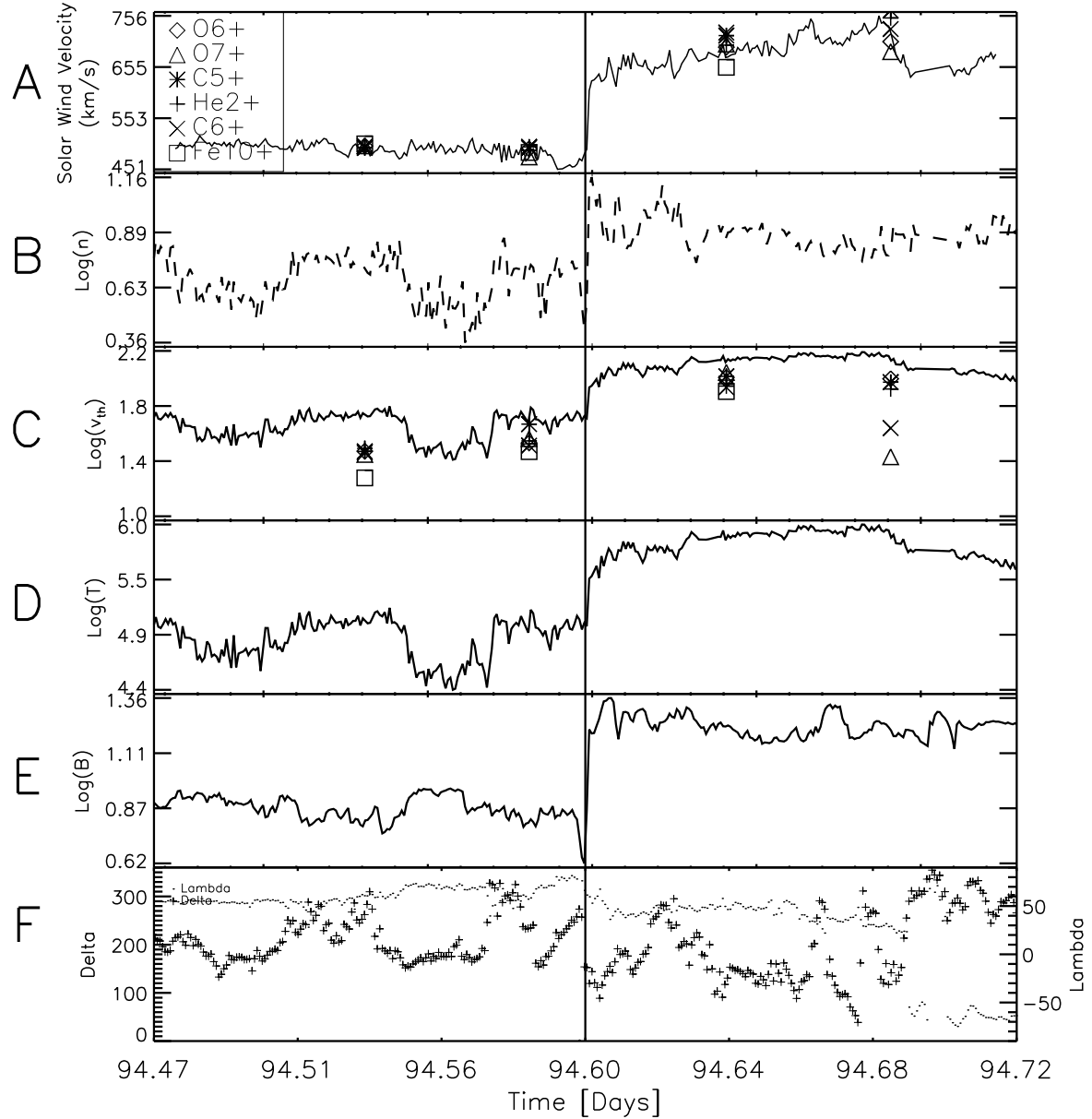


Fig. 1.— Plot of ACE magnetic and temperature data versus time, in fraction of a day, for a parallel shock. Panel A plots the solar wind proton velocity, v_p as the solid line and the velocity of each heavy ion is included as a different symbol. Panel B is plot of the proton number density, n . Panel C is a plot of the thermal velocity, v_{th} , of protons with the symbols representing the thermal velocity of individual heavy ions. Panel D plots the proton temperature, T , versus time. Panel E contains the magnitude of the magnetic field, B . Panel F is a plot of the magnetic latitude, δ , and longitude, λ .

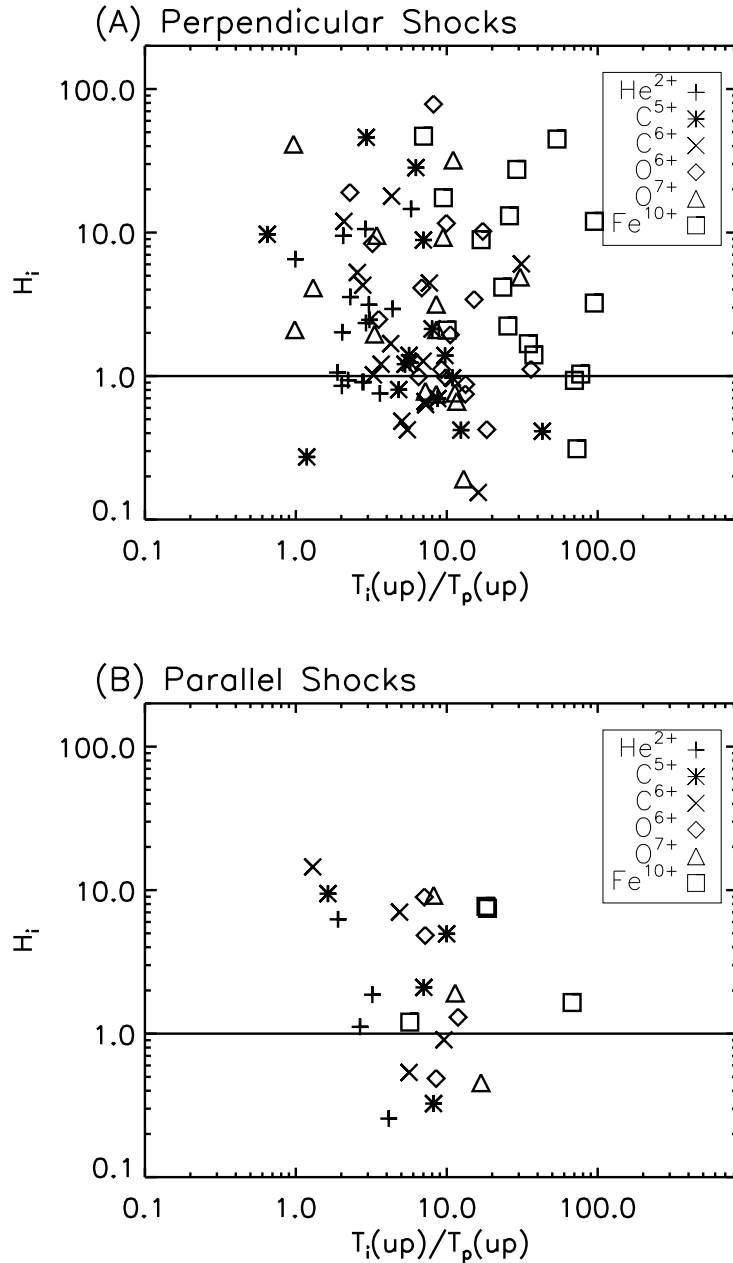


Fig. 2.— Shock ion heating versus upstream thermal temperature ratio, (a) for perpendicular shocks and (b) for parallel shocks. The upstream ratio of ion thermal velocity to proton thermal velocity, T_i/T_p , is the x-axis. Ion heating, H_i , is the y-axis.

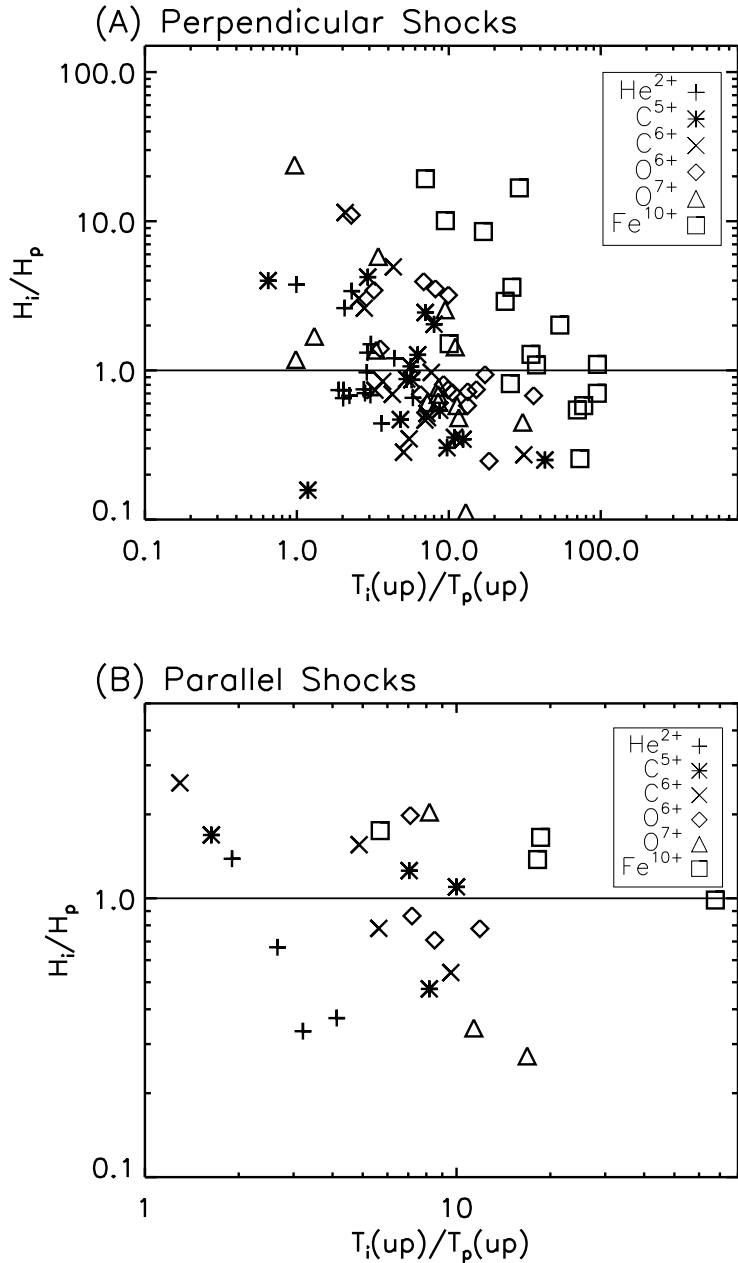


Fig. 3.— Shock heating ratios versus upstream thermal temperature ratio, (a) for perpendicular shocks and (b) for parallel shocks. The upstream ratio of ion temperature to proton temperature, T_i/T_p , is the x-axis. The ratio of temperature increase between the ion, H_i is the y-axis.

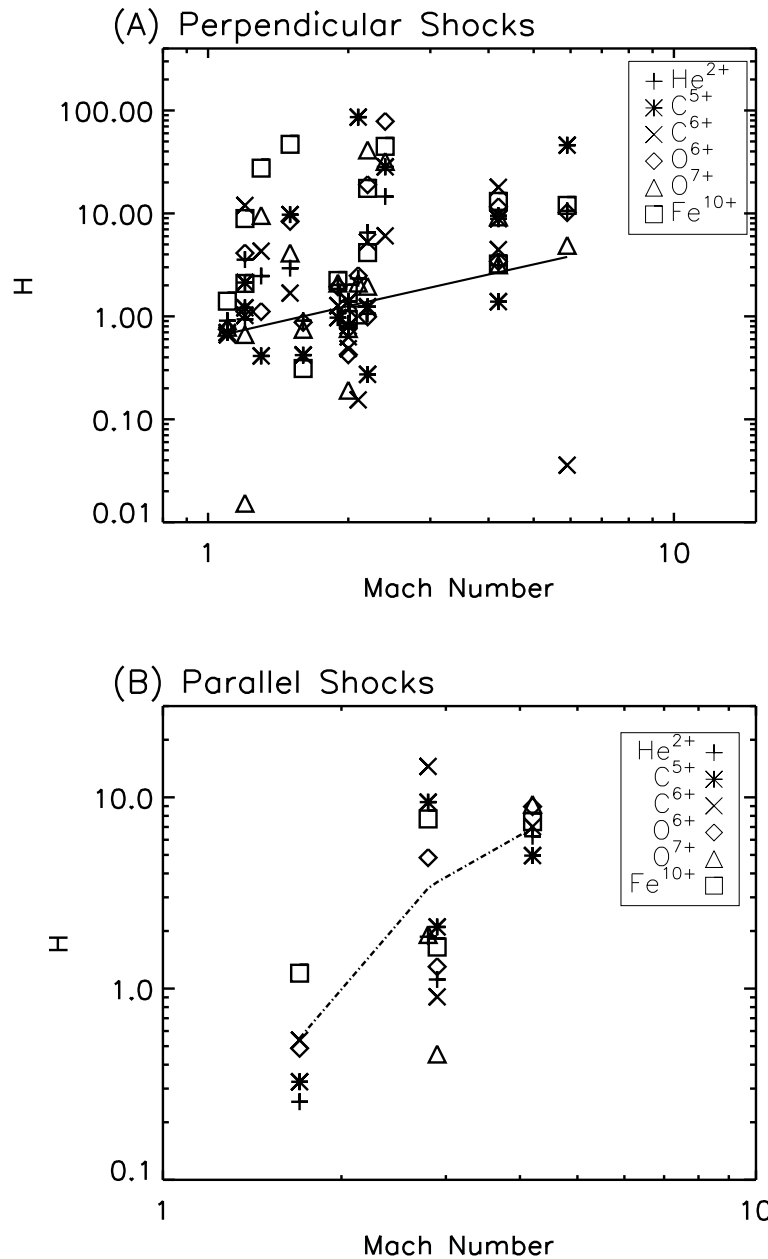


Fig. 4.— Plot of Alfvénic Mach number versus heating, H , for all the heavy ions. The line indicates a least squared fit to the data which appears kinked due to the logarithmic scale.

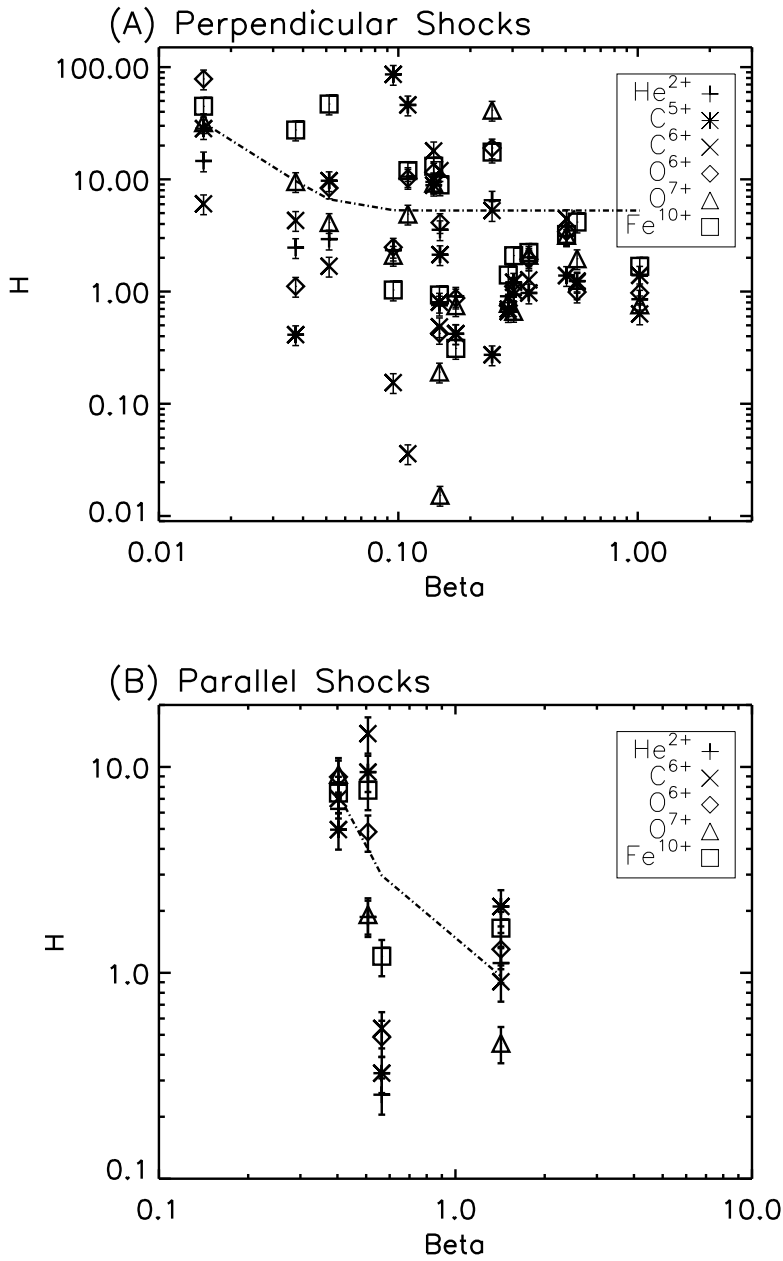


Fig. 5.— Plot of β versus heating, H , for all the heavy ions in a shock. The heating is the ratio of the square of the downstream ion thermal velocity to the square of the upstream ion thermal velocity. β is the ratio of thermal to magnetic energy densities. The line is the exponential fit to the data.

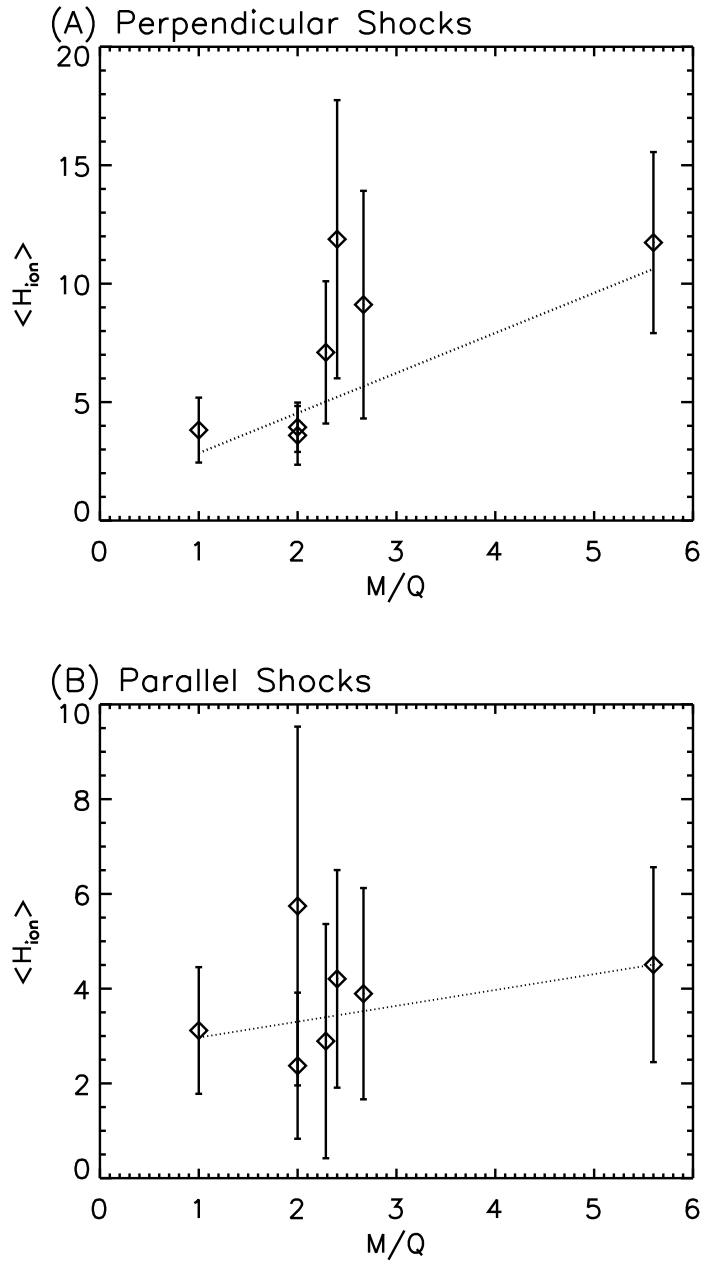


Fig. 6.— Plot of M/Q versus heating, H , for all the ions in a shock. The heating is the ratio of the square of the downstream ion thermal velocity to the square of the upstream ion thermal velocity. The heating for each ion was averaged in order to determine a trend in the data. The line is the least square fit to the data.